Detection and Analysis of Inter-Area Oscillations Through a Dynamic-Order DMD Approach

Annalisa Liccardo, Salvatore Tessitore, Francesco Bonavolontà, Sara Cristiano, Luigi Pio Di Noia, *Senior Member, IEEE*, Giorgio Maria Giannuzzi, and Cosimo Pisani

***Abstract*— This article deals with a novel method for detecting and analyzing inter-area oscillations on electric power transmission networks. The method starts from the modal analysis performed by the dynamic mode decomposition (DMD) algorithm, which is able to exploit the synchronized acquisitions of various measurement instruments to detect the mode of a dynamic system. Compared with the classical algorithm, the proposed method presents a fundamental improvement, which ensures its reliability even without having prior information on the type of input signal. In particular, the order of the DMD, i.e., the number of modes characterizing the acquired signal, is dynamically updated according to its energy content. The method has been tested with simulated signals, considering both single-oscillation signals and two-oscillation signals, varying the amplitude, frequency, and damping of the oscillatory components. In this way, the improvement with respect to the classical DMD was highlighted and the performance in terms of deviation between the estimated and nominal parameters was evaluated. Furthermore, the assessment on real life acquired signals has been performed; the results confirmed the reliability and accuracy of the measurement method, even in the presence of noisy signals and ambient data.**

***Index Terms*— Dynamic mode decomposition (DMD), dynamic order, inter-area oscillations, transmission grid stability.**

I. Introduction

THE energy transition that is currently underway is causing profound changes in the world electrical systems. The electricity transmission system is among the most involved in this change. In fact, the reliability and robustness of the transmission network is a fundamental prerequisite for the national and international exchange of the increasing quantities of electrical energy.

One of the phenomena that jeopardizes the stability of the transmission grid is the rotor angle stability [1]. It consists of the oscillatory transients that occur between long-distance generation systems whenever the balance between the generated power and the power demand changes [2], [3]. These transients appear on the transmission grid as frequency oscillations, called inter-area oscillations, characterized by an extremely low-oscillation frequency (typically between 0.1 and 0.4 Hz) [4]. The variation of the grid frequency can lead to the instability of the transmission system, since it can cause the out of step of the generators or the intervention of protection devices; these events produce, in turn, further transients, with a domino effect that, if not stopped, can lead to the power down of a section of the grid [5].

One of the crucial tasks of a transmission system operator (TSO) is the monitoring of the grid frequency to: 1) promptly detect the presence of oscillations; 2) evaluate the associated risk for the grid stability; and 3) undertake, if necessary, the appropriate countermeasures [6]. For this reason, the Italian TSO, Terna, constantly monitors the electrical quantities of the Italian transmission grid, through a wide area monitoring system (WAMS) [7], [8]. The measurement instruments of the WAMS are the phasor measurement units (PMUs), which are synchronized with each other through GPS, and measure and transmit the phasors of voltage and current, the measured frequency, the rate of change of the frequency, and eventual other analog and digital signals [9], [10]. To ensure the stability of the network, the raw data must be appropriately processed; so it is essential to invest in research and development of high-performance and reliable measurement methods, which processes the WAMS measurements to carry out an effective low-frequency oscillation analysis.

In this article, a novel method is proposed, based on an optimization of the traditional dynamic mode decomposition (DMD). The DMD processes the frequency measurements provided by WAMS and performs a modal analysis, to identify the main oscillatory modes characterizing the system state [11]. A joint research group from Terna Rete Italia and the Electrical and Electronic Measurements group of the University of Naples Federico II, worked to deeply characterize this approach and develop a strategy to determine the optimal energy threshold, according to which the DMD algorithm recognizes the significant modes immersed in the measurements provided by the WAMS. Compared with traditional modal analysis, the proposed approach is able to adapt to the input signal, because it dynamically detects the effective number of oscillations involved in the acquired measurements, without requiring *a priori* information.

This article is organized as follows: in Section II the most adopted methods for the analysis of inter-area oscillations are described; in Section III, a theoretical background on the DMD approach is provided; the proposed method is described in

Manuscript received 23 March 2022; revised 30 May 2022; accepted 9 June 2022. Date of publication 4 July 2022; date of current version 14 July 2022. The Associate Editor coordinating the review process was Dr. Yau Chung. *(Corresponding author: Annalisa Liccardo.)*

Annalisa Liccardo, Francesco Bonavolontà, and Luigi Pio Di Noia are with the Department of Electrical Engineering and Information Technology, University of Naples Federico II, 80125 Naples, Italy (e-mail: annalisa.liccardo@unina.it; francesco.bonavolonta@unina.it; sara.cristiano@unina.it; luigipio.dinoia@unina.it).

Salvatore Tessitore, Sara Cristiano, Giorgio Maria Giannuzzi, and Cosimo Pisani are with Terna Rete Italia, 00156 Rome, Italy (e-mail: salvatore.tessitore@terna.it; sara.cristiano@terna.it; giorgio.giannuzzi@terna.it; cosimo.pisani@terna.it).

Digital Object Identifier 10.1109/TIM.2022.3186371

Section IV-B; in Sections V and VI results obtained during the method assessment with synthesized signals and real WAMS acquisitions, respectively, are presented; in Section VII some concluding remarks are discussed.

II. Measurement of Inter-Area Oscillations

The typical method for inter-area oscillation analysis consists of modeling the frequency signal as a damped oscillation, or the composition of multiple damped oscillations, according to the formula

$$x(t) = \sum_{i=1}^{N} A_i e^{-\sigma_i t} \sin 2\pi f_i t. \tag{1}$$

The parameters A_i, σ_i, and f_i, which are, respectively, amplitude (in Hz), damping (in s^{-1}), and frequency (in Hz) of the ith oscillation, are estimated as the parameters that best fit the input signal.

Amplitude, damping and frequency provide the necessary information to identify the type of oscillation and its dangerousness.

The amplitude estimation, first of all, allows to verify that the frequency oscillations remain below an alarm threshold, beyond which it is necessary to operate with corrective actions (such as load shedding) to preserve the stability of the network.

The study of the damping is also fundamental, since it allows to establish in advance the risk associated with the oscillation. A positive and high damping value indicates an oscillation that tends to extinguish rapidly, while if the damping is negative, the oscillation is characterized by increasing amplitude and should be counteracted. Even a weakly damped oscillation (with $\sigma < 0.05$) is considered a dangerous condition that should be monitored [2].

Frequency provides information about the type of oscillation. In particular, the historical measurements within the Continental European system show three main oscillation modes: the East-West mode, appeared following the Turkey connection, characterized by a frequency of about 0.15 Hz, the East-Center-West mode shows frequency around 0.2 Hz, the North-South mode, that exhibits a typical frequency near to 0.3 Hz [12], [13].

Therefore, it is clear that the skill in preserving network stability is closely related to the performance of the adopted measurement method. Several approaches are available in literature. Zamani *et al.* [14] have focused their attention on the so-called signal-based methods, that are those relying on the processing of signals coming from measurement instruments, rather than on the knowledge of the network model.

The most widely used method in the past was the Prony approach, based on the decomposition of the signal proper into a set of damped oscillations. This method, however, proved to be very sensitive to the noise affecting the analyzed signal [15], [16].

Among the methods that attempt to extend the Prony approach in the presence of noise [17], the Tufts–Kumaresan method is the best known [18], [19]. The characterizing modes of the system are identified through the study of the extraneous zeros of the system itself and the parameters characterizing these modes are estimated. The method shows remarkable accuracy in the estimation of frequency and damping, while it is less reliable as concerns to the estimation of amplitude.

Among the methods that do not require *a priori* information about the input signal, approaches based on Empirical Mode Decomposition should also be considered [20]. In the past, Bonavolontà *et al.* [21] and Lauria and Pisani [22] have also proposed a method based on this decomposition approach. The method is particularly suitable for non-stationary signals and provides very accurate frequency estimates. The main observed drawback, however, concerns the difficulty to correctly resolve near frequency oscillations. Considering that on the transmission system it is possible to detect simultaneously oscillations at 0.25 and 0.3 Hz, in these cases the method is not sufficiently accurate.

Heuristic methods (Particle Swarm Optimization, Genetic Algorithm) also perform well without requiring *a priori* information of the input signal [23], [24]. The problem with such methods is that rarely they converge on solutions that are very far from the actual ones, especially in the presence of noise. In critical applications, such as the monitoring of transmission network stability, the estimate of totally incorrect parameters, though if rarely occurs, can lead to bad decisions and must be avoided.

Kalman Filter-based methods are fascinating because of their flexibility and the ability to estimate the parameters of oscillations in real time; as new measurement data enter the algorithm, the estimates are updated [25], [26]. The performance of the method is highly dependent on the choice of initial values of the R and Q matrices. In addition, the computational load is not negligible, especially if multiple oscillations are to be determined. In some applications in literature, in fact, the computational load is reduced by limiting the analysis to a single dominant oscillation.

The methods based on wavelet transform (WT), provide promising results, especially with transient signals such as inter-area oscillations [27]. The problem, in this case, is the optimal choice of the time scale [28]. The WT, in fact, allows to privilege the temporal resolution at the expense of the frequency resolution and vice versa. In this case, the typical oscillations have very low frequencies and very close to each other (so it is required a notable frequency resolution); but it is also essential to locate in time the trend of oscillations to appreciate the consequences of countermeasures taken (so it is required also an equally high time resolution).

This same issue characterizes all methods based on time-frequency analysis. It is not possible to determine in advance if it is necessary to increase the frequency resolution (because there are more oscillations on the network) or the temporal resolution (because there is a predominant transient that must be monitored and counteracted).

All of the described methods are single-channel approaches, which process the data frame from a single measurement instrument. These approaches, therefore, are not very robust to the problems that can affect instrument measurements, as noise, missing measurements, and data transmission failure).

For this reason, the authors' attention has shifted to multi-channel methods, in which multiple signals, coming

from different measurement systems, are processed. Terna, in fact, monitors the transmission network through several synchronized PMUs that transmit the measurements to a central node, which aligns them temporally and stores them into a database. Thus, at a given instant of time, synchronized sets of measurements from all PMUs of the WAMS are available, and this can be exploited for more robust oscillation estimation.

In [29] a multi-channel extension of the WT is proposed, exploiting multiple signals from different measurement instruments. It has been observed, however, that the choice of algorithm parameters (choice of mother wavelet, center frequency, dilation, and translation) greatly affects the accuracy of the estimate. In [30], the Ibrahim time domain (ITD) method was applied to estimate the modes of oscillation. The algorithm is really robust to noise and has been tested on real PMUs measurements; unfortunately, to ensure good accuracy, a processing window of 5–10 min is required; these time windows are not compatible with the response times required to implement corrective maneuvers and preserve the system stability.

Cai *et al.* [31], Sarmadi and Venkatasubramanian [32], and Kutz *et al.* [33], thus, have identified approaches based on modal analysis as more reliable; among them, DMD is particularly promising since it is a data-driven approach, which does not approximate the system dynamics with a particular model, but it is based on the observation of experimental data. As it will be described, a crucial point of DMD is the order selection, which greatly affects the performance of the method. The authors propose a measurement method that is based on automatic order selection, chosen according with the characteristics of the input signal.

III. Fundamentals on DMD

The first rigorous formulation of the DMD algorithm is due to Peter Schmidt and Jörn Sesterhenn, who in 2008 defined the algorithm and demonstrated how it was able to recognize the nonlinear dynamics of fluid motion by having photographs over time of a set of measurements taken at different points in the fluid [34], [35].

The DMD is based on the local approximation of a dynamic system with a linear system, which can be described by the system of differential equations

$$\frac{d\mathbf{x}}{dt} = \mathcal{A}\mathbf{x} \tag{2}$$

whose solution is

$$\mathbf{x}(t) = \sum_{k=1}^{n} \phi_k e^{\omega_k t} b_k = \Phi e^{\Omega t}\mathbf{b}. \tag{3}$$

The components of $\mathbf{x}(t)$ are the dynamic modes of the system. The terms ϕ_k and ω_k are, respectively, the eigenvectors and eigenvalues of the dynamic matrix $\mathcal{A}$, while the coefficients b_k represent the coordinates of the initial value $\mathbf{x}(0)$ in the base of the eigenvectors.

In the presence of discrete-time representation of the system, (2) is expressed by the following formula:

$$\mathbf{x}_{k+1} = \mathbf{A}\mathbf{x}_k \tag{4}$$

where $\mathbf{A} = e^{\mathcal{A}\Delta t}$ and Δt is the sampling time.

Consider, now, to have m snapshots of a system, taken at different time instants, each Δt. For $i = 1, \ldots, m$, each snapshot is a vector $[x_{1,i}, x_{2,i}, \ldots, x_{n,i}]$ containing n spatially distributed measurements in the system. It is possible to arrange the data by constructing the two matrices

$$\mathbf{X}_1 = \begin{bmatrix} x_{1,1} & x_{1,2} & \ldots & x_{1,m-1} \\ x_{2,1} & x_{2,2} & \ldots & x_{2,m-1} \\ \vdots & \vdots & \ddots & \vdots \\ x_{n,1} & \ldots & \ldots & x_{n,m-1} \end{bmatrix} \tag{5}$$

$$\mathbf{X}_2 = \begin{bmatrix} x_{1,2} & x_{1,3} & \ldots & x_{1,m} \\ x_{2,2} & x_{2,3} & \ldots & x_{2,m} \\ \vdots & \vdots & \ddots & \vdots \\ x_{n,2} & \ldots & \ldots & x_{n,m} \end{bmatrix}. \tag{6}$$

The local approximation of (4) can be written as follows:

$$\mathbf{X_2} = \mathbf{A}\mathbf{X_1}. \tag{7}$$

Therefore, the matrix $\mathbf{A}$ can be determined according to

$$\mathbf{A} = \mathbf{X}_2\mathbf{X}_1^{\dagger} \tag{8}$$

where $\mathbf{X}_1^{\dagger}$ is the pseudo-inverse of $\mathbf{X}_1$.

The knowledge of $\mathbf{A}$ allows to derive the eigenvalues and, consequently, the parameters that characterize the dynamic modes of the system. The problem is that often the dimension of the matrix $\mathbf{A}$ is considerable and it is complicated to represent all the modes in which the system is decomposed. Considering that in the system the number of significant modes is low if compared to the size of the matrices, the DMD does not estimate all the eigenvalues of the matrix $\mathbf{A}$, but those of a reduced-rank matrix $\tilde{\mathbf{A}}$, which approximates the most significant part of $\mathbf{A}$. For the determination of $\tilde{\mathbf{A}}$, the factorization technique called singular value decomposition (SVD) is used. The SVD is adopted to decompose the $n \times m-1$ matrix $\mathbf{X}_1$, according to this formula

$$\mathbf{X}_1 = \mathbf{U}\Sigma\mathbf{V}^{\star} \tag{9}$$

where $\mathbf{U}$ is an $n \times n$ unitary square matrix; Σ is an $n \times m$ rectangular diagonal matrix with non-negative real numbers on the diagonal; $\mathbf{V}^{\star}$ is the conjugate transpose of $\mathbf{V}$, that is an $m \times m$ unitary matrix. The matrices $\mathbf{U}$ and $\mathbf{V}$ are also orthogonal.

The elements of Σ are called singular values of $\mathbf{X}_1$; each column of $\mathbf{U}$ is called left singular vector, while each column of $\mathbf{V}$ is called right singular vector. The SVD, in practice, performs the decomposition of a matrix with respect to the orthonormal basis consisting of the columns of $\mathbf{U}$. The singular values represent the components of $\mathbf{X}_1$ in this basis.

Singular values are characterized by the following property:

$$s_i \geq 0 \quad and \quad s_i \geq s_{i+1} \quad \forall i = 1, \ldots, n. \tag{10}$$

This means that the singular values are arranged in the matrix Σ in descending order; for the physical meaning of singular values, this means that the diagonal of Σ gives the components of $\mathbf{X}_1$ on the orthogonal basis of $\mathbf{U}$ in order of importance.

Actually, in the proposed measurement method the truncated SVD is exploited, which is preferred when the input matrix

$\mathbf{X_1}$ is rectangular. It can be demonstrated that the rank r of Σ is equal to the rank of the matrix being decomposed; so, if the input matrix is rectangular, the number of non-zero singular values would be, at most, equal to the smaller of the dimensions between n and m. The truncated SVD directly constructs a square matrix Σ with dimension equal to the rank r. The decomposition is performed according to this formula

$$\mathbf{X}_{1(n\times m-1)} = \mathbf{U}_{(n\times r)}\Sigma_{(r\times r)}\mathbf{V}^{\star}_{(r\times m-1)}. \tag{11}$$

If the decomposition in (9) is used to replace $\mathbf{X_1}$, (8) becomes

$$\mathbf{A} = \mathbf{X}_2\mathbf{V}\Sigma^{-1}\mathbf{U}^{\star}. \tag{12}$$

Instead, if the truncated SVD is adopted, the matrices with reduced rank r are obtained from (11); so, the reduced rank $\tilde{\mathbf{A}}$ can be determined directly in the orthogonal basis $\mathbf{U}$

$$\tilde{\mathbf{A}} = \mathbf{U}\mathbf{A}\mathbf{U}^{\star} = \mathbf{U}^{\star}\mathbf{X}_2\mathbf{V}\Sigma^{-1}. \tag{13}$$

The eigenvalues and eigenvectors of the matrix $\tilde{\mathbf{A}}$ provide the dominant modes of the system, the number of which will be r. It is worth noting, however, that for sufficient knowledge of the system, it may not be necessary to evaluate all the modes. The singular value matrix, as mentioned, shows the components of the input matrix in the orthogonal basis $\mathbf{U}$, in order of amplitude. It is possible to decide, therefore, to consider a small number of singular values. This can be achieved by reducing the matrices $\mathbf{U}$, Σ and $\mathbf{V}$. In particular, if only p modes are desired to represent the input matrix $\mathbf{X}_1$, with $p < r$, the matrix of singular values will be Σ_p, that is a $p \times p$ square matrix having on the diagonal the first p values of Σ_r. The matrices $\mathbf{U}_p$ and $\mathbf{V}_p^{\star}$ will have dimension $n \times p$ and $p \times m-1$, respectively, and p is called order of the DMD.

To efficiently explain the meaning of the DMD order and the effect of the reduction of the matrices $\mathbf{U}$, Σ, and $\mathbf{V}$, an example based on image analysis is considered. The general input matrix $\mathbf{X}$ is the matrix of pixels of the black and white image shown in Fig. 1(a), taken among the test images provided by the MATLAB environment [36]. The size of $\mathbf{X}$ is 246×300. Applying SVD to the matrix $\mathbf{X}$, the matrices $\mathbf{U}$, Σ, and $\mathbf{V}$ of size, respectively, 246×246, 246×246, and 300×246 are obtained.

Fig. 1(b)–(d) show the images reconstructed by reducing the rank of the matrix Σ to 50, 30, and 10, respectively. It can be observed that if only the first 50 singular values are considered, i.e., a compression ratio of about 80% is applied, the information content of the image is still intact. If the rank is reduced to 30 (compression ratio equal to 88%), part of the information is lost; it is feasible to understand that the image represents coins, but it is not possible to distinguish the surface to understand the type of coins. Finally, if only ten singular values are considered (96% compression ratio) the image is strongly degraded. It is possible to identify the edges of the objects and their number, but it is impossible to understand what kind of object is represented in the image.

This result shows that it is certainly possible to work with reduced-rank matrices without losing necessary information, but it is crucial to identify the appropriate order of the DMD, i.e., the rank to which the singular matrix will be truncated and, consequently, the rank of the matrix $\tilde{\mathbf{A}}$ with which the dynamics of the system will be represented.

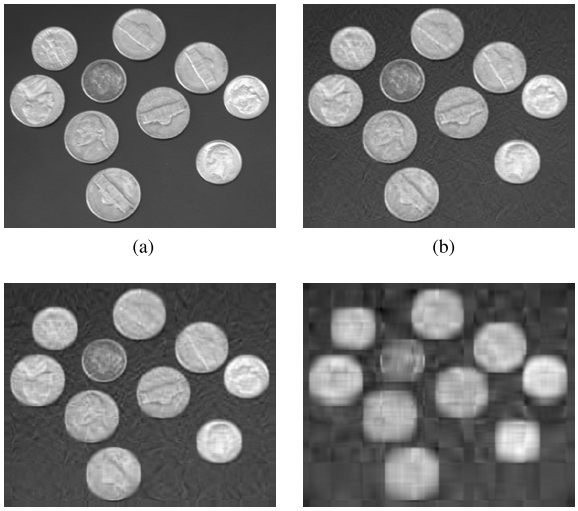

Fig. 1. Reconstructed input image with different ranks of the matrix Σ_p. (a) Original input image. (b) $p = 50$. (c) $p = 30$. (d) $p = 10$.

IV. Proposed Method

A. DMD Optimization With Dynamic Order

In the classical DMD approach, the order is *a priori* established, based on the information content that is desired. It is clear, however, that one value of the order is not necessarily the optimal one for all scenarios. If the order is too low, fundamental information may be lost. Conversely, if the order is too high compared to the salient information, the algorithm may also return artifacts due to the request to model the system with more components than that really significant. This last aspect will be fully clarified in Section V, where DMD will be applied to a synthesized signal, characterized by a reduced number of oscillatory modes.

The authors, therefore, considered the algorithm, hereafter referred to as dynamic-order DMD [11], [37], capable of automatically adapting the order according to the signal to be processed.

In particular, the method is based on the estimation of the parameter called cumulative sum of singular value (CSSV), evaluated as

$$\mathrm{CSSV}(p) = \frac{\sum_{i=1}^{p} s_i}{\sum_{i=1}^{r} s_i} \tag{14}$$

where s_i is the ith singular value, r is the rank of the matrix Σ_r obtained by the truncated SVD, and $p = 0, \ldots, r$. The CSSV represents the cumulative sum of the amplitudes of the singular values, related to the total sum.

In Fig. 2 the evolution of the CSSV parameter of the image of Fig. 1(a) is shown. It can be seen from the figure that most of the information content resides in the first singular values. In particular, the image in Fig. 1(b) reconstructed with the SVD order of 50 holds the 83% of the information provided by the singular values. If the 97% of the information content is desired, the order cannot be less than 127.

The use of the CSSV parameter, therefore, allows to set *a priori* the desired percentage of information content; the

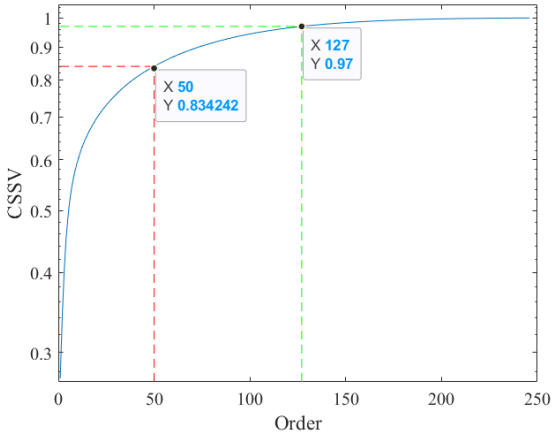

Fig. 2. CSSV evolution in dependence on the rank p.

order, i.e., the rank p at which the dynamic matrix will be approximated, is established *a posteriori*, on the basis of the obtained singular values of the input matrix decomposition.

The selection of the threshold, however, is not a trivial step; in some scenarios, the operator is interested in one main component, in other cases, where energy is spread over multiple components, the operator want to observe all components excluding noise. For this reason, a large part of the activity consisted in identifying the optimal threshold, through an intensive characterization of the method on synthetic and real data.

B. Method for the Estimation of the Oscillations Parameters

In this section, the whole proposed measurement method is shown to make it applicable to the measurement data coming from the WAMS of the transmission network. The data coming from the PMUs are organized into 20-s time windows. This choice is dictated by the trade-off between a low-response time of the algorithm and the need to have a sufficient number of cycles of the oscillatory signals to correctly estimate its parameters. At the expected minimum frequency of 0.1 Hz, 2 periods of the signal would be observed in a 20-s window. The PMU measurements are transmitted at a rate of 50 frames per second (fps), so, the processing window contains 1000 samples.

The samples of the window are preliminary arranged to provide them as input to the measurement algorithm. In particular, missing data, due to possible transmission problems, are searched and estimated by interpolation with a moving average algorithm.

Subsequently, the signal is filtered using a Hilbert-type FIR filter with a bandwidth characterizing the frequency range of inter-area oscillations. In this way, any unwanted frequency components are excluded from the analysis. To limit the edge effects of the filter, the boundaries of the time window are extended by adding 500 samples at the start and at the end of the processed array; after filtering, the subset of the central 1000 samples is taken as filtered data.

At this point, the matrix $\mathbf{X}$ to be processed with DMD has dimension $n \times m$, where n is the number of PMUs and m is the number of sampling instants of the time window (1000). The generic entry x_{ij} is the frequency measurement performed by the ith PMU in the jth sampling instant.

Matrices $\mathbf{X}_1$ and $\mathbf{X}_2$ are constructed, both of $m-1$ columns; $\mathbf{X}_1$ has columns of $\mathbf{X}$ ranging from 1 to $m-1$; $\mathbf{X}_2$ has columns of $\mathbf{X}$ ranging from 2 to m. The truncated SVD is performed on matrix $\mathbf{X}_1$, according to (11), obtaining the matrices $\mathbf{U}$, Σ, and $\mathbf{V}^\star$.

The CSSV parameter of the singular values is estimated and the order of the DMD p is determined when the 97% threshold is exceeded. The reduced matrices $\mathbf{U}_p$, Σ_p, and $\mathbf{V}_p^\star$ are then determined.

Once the matrix $\tilde{\mathbf{A}}$ is obtained through (13), the spectral decomposition is performed according to

$$\tilde{\mathbf{A}}\mathbf{W} = \mathbf{W}\Lambda \tag{15}$$

where $\mathbf{W}$ is a matrix whose columns are the eigenvectors of $\tilde{\mathbf{A}}$ and Λ is a diagonal matrix, which contains the corresponding eigenvalues λ_k.

At this point it is possible to reconstruct the characteristic modes of the system and, then, estimate all the parameters of (19). The columns ϕ_k of the matrix Φ, called DMD modes, are the eigenvectors reported from the orthogonal basis $\mathbf{U}$ to the representation space

$$\Phi = \mathbf{X_2}\mathbf{V}\Sigma^{-1}\mathbf{W}. \tag{16}$$

The eigenvalues of the dynamic matrix $\mathcal{A}$, indicated as ω_k, are derived from the eigenvalues of $\tilde{\mathbf{A}}$ through the formula

$$\omega_k = \frac{\ln \lambda_k}{\Delta t}. \tag{17}$$

The eigenvalues of $\mathcal{A}$ are both real and complex numbers. Since the modes to be detected are the damped oscillatory modes, the algorithm selects only pairs of complex and conjugate eigenvalues. In this case, the real part represents the damping of the oscillation, while the imaginary part, divided by 2π, gives the frequency of the oscillatory component. The algorithm, makes a further sifting, selecting only the modes characterized by the frequency that falls in the range of interest between 0.1 and 0.4 Hz.

Finally, to derive the value of the coefficients b_k, the state vector $\mathbf{x}(0)$ at time $t = 0$ has to be evaluated. Equation (3), when $t = 0$ becomes $\mathbf{x}(0) = \Phi\mathbf{b}$. Therefore,

$$\mathbf{b} = \Phi^{-1}\mathbf{x}(0). \tag{18}$$

V. Assessment on Synthesized Signals

To assess the performance of the proposed method, tests on synthesized signals have been preliminarily performed in MATLAB environment. The data coming from the WAMS have been emulated, so a set of signals have been synthesized consisting of one or two damped oscillations, characterized by frequencies close to those expected on the transmission network. The frame containing the frequency measurements is 25-min long and the sampling rate is 50 S/s. The DMD algorithm works with snapshots containing spatially distributed measurements; so, it was necessary to simulate a set of measurements provided from different PMUs located at different points of the network. To obtain correlated signals, a constant phase displacement has been applied. The phase

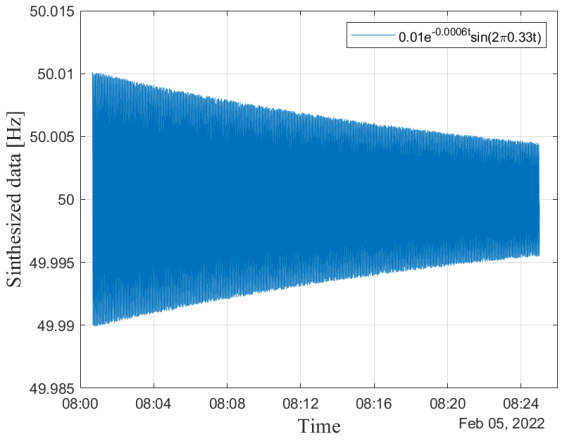

Fig. 3. Synthesized single-oscillation signal.

shift was achieved by imposing a time delay of 0.6 s. Therefore, the simulated signal for each PMU is described by the equation

$$x_i(t) = Ae^{-\sigma t} \sin(2\pi f t + 2\pi f 0.6\, i) \tag{19}$$

where i =1,…,10 is the PMU number.

The signals, then, were corrupted with Gaussian noise associated with a signal-to-noise ratio (SNR) of 40 dB.

In all the performed tests, the estimates of the classical DMD algorithm were compared with those provided by the proposed method. It should be noted that the classical DMD algorithm was configured to detect three main oscillations. In several tests, it has been observed that the optimal order of the DMD should be set equal to twice the expected number of modes increased by two. This is because each mode is described by two complex, conjugate eigenvalues of the dynamic matrix $\mathcal{A}$. The other two eigenvalues are needed to describe modes with which the response of the used digital filter is modeled. Therefore, in the classical DMD algorithm, the singular value matrix is truncated to the order p equal to 8. The proposed method with dynamic order DMD has been configured to set the order in correspondence of a CSSV greater than 0.97.

As an example, the synthesized signal, shown in Fig. 3 is considered. It consists of a single oscillation, characterized by amplitude A equal to 0.01 Hz, frequency f equal to 0.33 Hz and damping σ equal to 0.0006 s^{-1}.

In Fig. 4, the frequency, amplitude, and damping estimated by the classical DMD algorithm at the sampling rate of 50 S/s are shown, respectively. From Fig. 4(a), it can be seen that the 0.33-Hz frequency of the set oscillatory mode is determined correctly in almost all time windows. Having configured the algorithm to search for three oscillatory modes, two more modes of frequency varying around 0.25 and 0.18 Hz are returned. These modes are artifacts, probably related to the frequency response of the filter which, not being perfectly flat, in the presence of noise tends to amplify some frequencies and attenuate others. The presence of these two fictitious modes creates a mode mixing problem; in Fig. 4(a), at t = 8:17 it can be noted that the frequency of 0.33 Hz is attributed to mode 2, because a mode with a higher frequency, equal to about 0.34 Hz, is identified as mode 1.

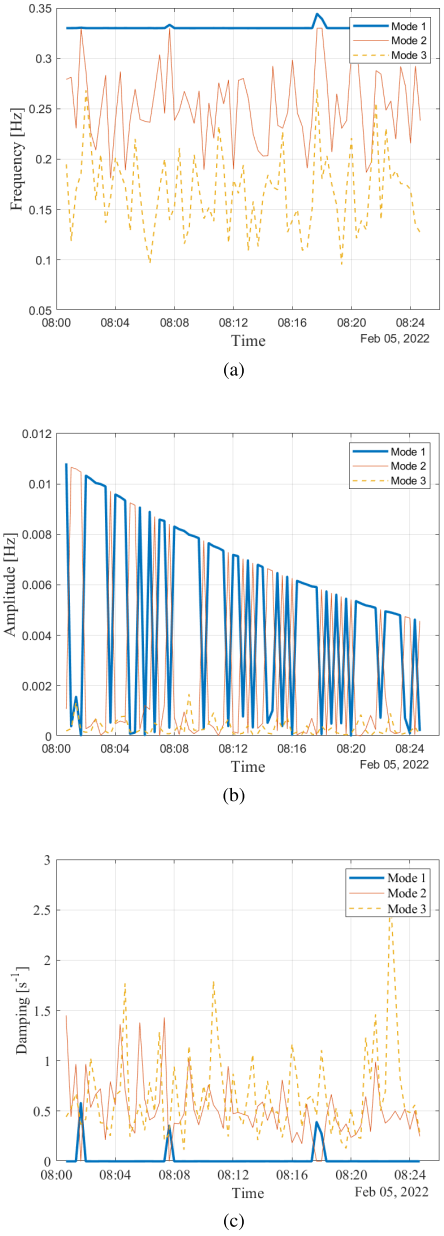

Fig. 4. Estimated parameter from a single-oscillation signal with the classical DMD. (a) Estimated frequency. (b) Estimated amplitude. (c) Estimated damping.

The phenomenon of mode mixing is even more evident on the estimated amplitudes in Fig. 4(b). The initial amplitude of the simulated mode is estimated to be 0.0108 Hz, with a deviation of 8% from the nominal value. However, this amplitude is attributed in some windows to mode 1 and in others to mode 2, making the information difficult to understand.

As for the damping in Fig. 4(c), mode mixing is also observed here in some cases. In any case, the mode 1 damping is estimated to be 0.0003, with a 50% deviation from the nominal value; the estimated damping for the other two modes is not significant and, in fact, exhibits very high values compared to typical real conditions.

The same signal has been analyzed by means of the proposed dynamic-order DMD, obtaining the results shown in Fig. 5. It can be seen that the algorithm correctly recognizes

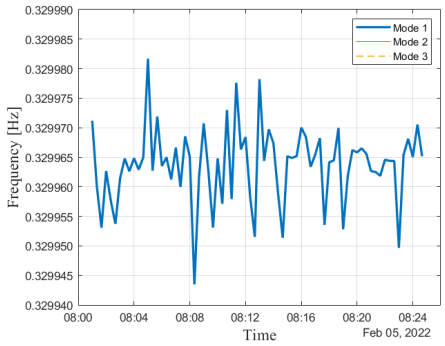

(a)

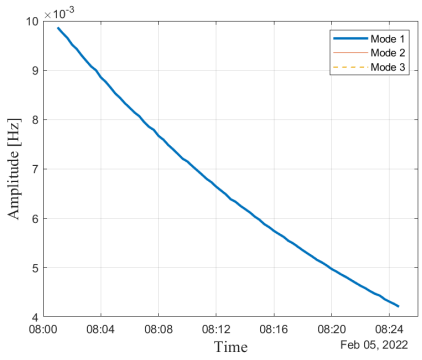

(b)

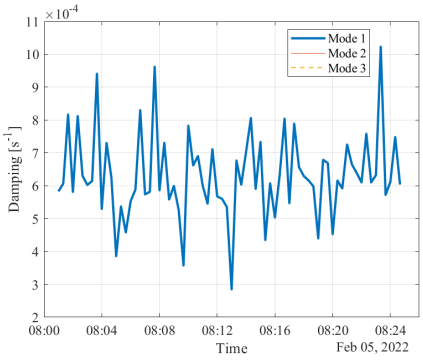

(c)

Fig. 5. Estimated parameter from a single-oscillation signal with the proposed method. (a) Estimated frequency. (b) Estimated amplitude. (c) Estimated damping.

only one dominant mode, of which it estimates amplitude frequency and damping with excellent accuracy. In fact, the maximum deviation between the estimated and nominal frequency is 60 μHz. The initial estimated amplitude of the oscillation is 0.00987 Hz, with a deviation of 1.3% from the nominal value. Regarding the damping, the maximum deviation between estimated and nominal value is 4×10^{-4} s^{-1}; in particular, the mean estimated value in all windows is 5.99×10^{-4} s^{-1} and the standard deviation is 0.95×10^{-4} s^{-1}.

A particularly significant signal, which shows the better performance of the proposed algorithm compared to classical DMD, is shown in Fig. 6. The synthesized signal consists of two damped oscillations: the first, divergent, characterized by amplitude equal to 0.02 Hz, frequency of 0.3 Hz, and damping equal to -0.001 s^{-1}; the second is characterized by amplitude equal to 0.05 Hz, frequency of 0.2 Hz and damping equal to

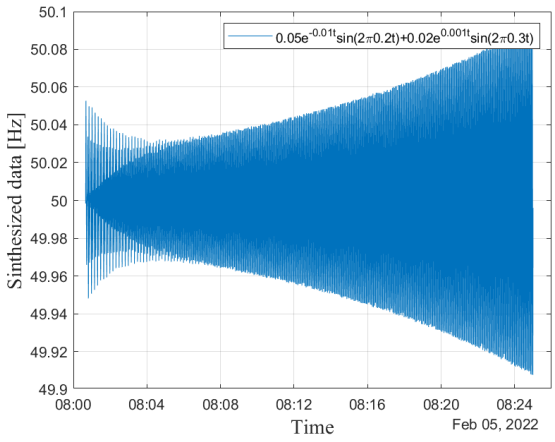

Fig. 6. Synthesized two-oscillation signal.

0.01 s^{-1}. The order of the classical DMD was set equal to 6. The results provided by the classical DMD are shown in Fig. 7.

It can be seen that in the first part of the frame, the DMD correctly estimates frequency, amplitude and damping, since the considered order is the optimal one to detect two oscillations within the signal. When, however, the first oscillation is completely damped and, therefore, the signal is composed of only one divergent oscillation, the order equal to 6 is no longer adequate and the algorithm again shows mode mixing problems in the amplitude estimates.

Fig. 8 shows the results obtained from dynamic-order DMD. In this case, it can be noted that the order is automatically modified by the algorithm during window processing. In fact, two modes are recognized until time 8:10. Successively, the second oscillation decays and does not contribute to the signal energy anymore. Therefore, when the dynamic-order algorithm processes the 20-s windows, the main energy contribution is given only by the 0.3-Hz oscillation; the estimated order becomes equal to four and the parameters of only one oscillation are estimated.

The frequency estimates are very accurate, as observed in all the performed tests; the worst condition is observed in the interval where mode 2 is extinguishing, where the frequencies of the mode 2 is estimated to be 0.192 Hz. In the remaining intervals, the maximum deviation between estimated and nominal frequency is 50 μHz for both the modes.

Also the amplitudes are estimated with notable accuracy; in particular the amplitude of the first mode is estimated equal to 0.0203 Hz, the amplitude of the second mode is equal to 0.0483 Hz. Finally, as far as damping is concerned, the estimate of the first mode varies around -9.7×10^{-4} s^{-1} and that of mode 2 varies around 10×10^{-3} s^{-1}. Also for the damping, estimates worsen in the time interval when mode 2 is extinguishing.

The proposed method was tested on several types of signals, varying frequencies, amplitudes, and damping of the oscillations, to obtain a global indication of the performance of the method on simulated signals. In particular, a set of experiments was first performed in which the synthesized signal consisted of a single oscillation; the amplitude was varied, with logarithmic step, between 0.01 and 0.5 Hz, the frequency was varied

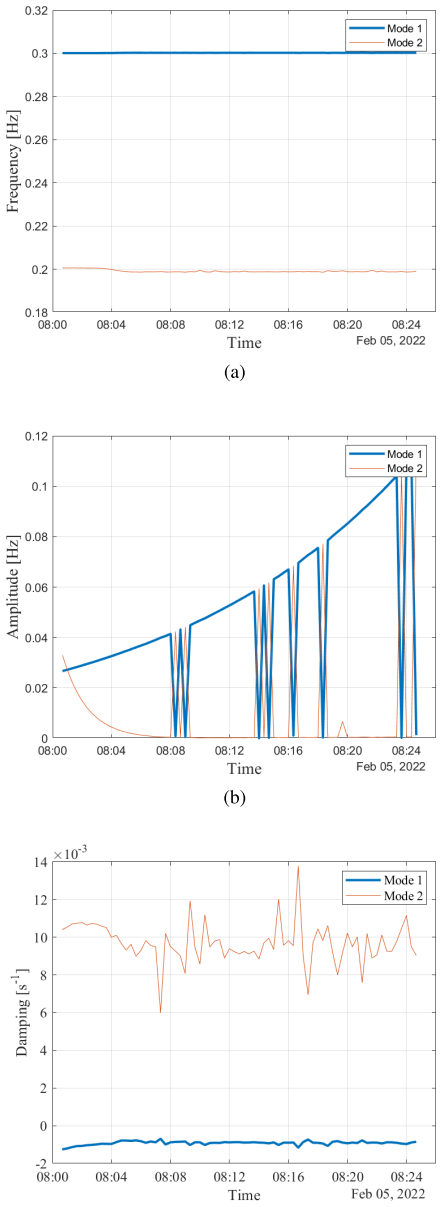

Fig. 7. Estimated parameter from a two-oscillation signal with the classical DMD. (a) Estimated frequency. (b) Estimated amplitude. (c) Estimated damping.

with linear step between 0.15 and 0.35 Hz and the damping was changed with logarithmic step between 0.001 and 0.01, both with positive and negative values. For the frequency, amplitude, and damping estimates, percentage deviations from the nominal value were evaluated according to the formulas

$$\begin{aligned} \Delta f_{\%} &= 100 \cdot \frac{\hat{f} - f}{f} \\ \Delta A_{\%} &= 100 \cdot \frac{\hat{A} - A}{A} \\ \Delta \sigma_{\%} &= 100 \cdot \frac{\hat{\sigma} - \sigma}{\sigma} \end{aligned} \tag{20}$$

where $\hat{f}$, $\hat{A}$, and $\hat{\sigma}$ are the estimates of frequency, amplitude and damping, respectively, while f, A, and σ are the nominal values.

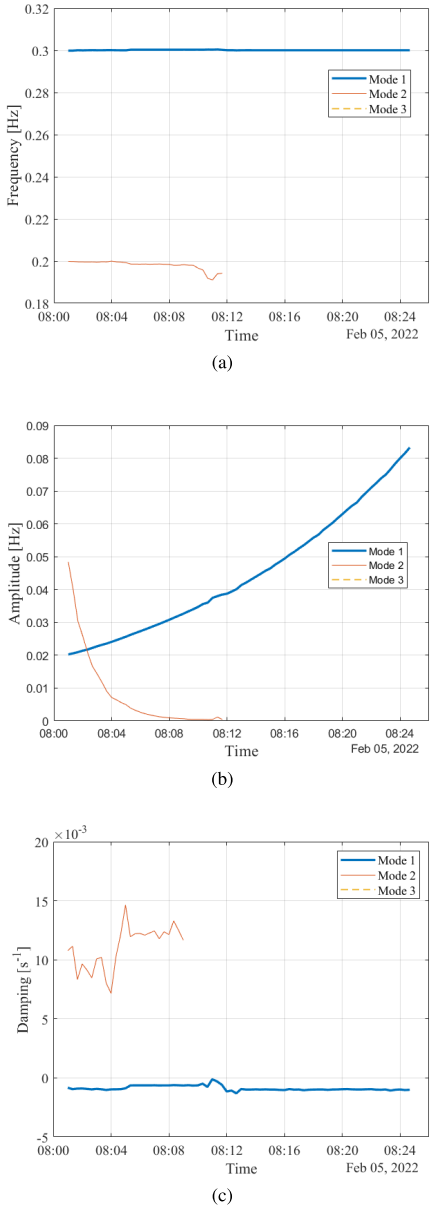

Fig. 8. Estimated parameter from a two-oscillation signal with the proposed method. (a) Estimated frequency. (b) Estimated amplitude. (c) Estimated damping.

The deviation observed in the frequency estimates are shown in Fig. 9. It can be noted that the proposed method estimates the frequency with excellent accuracy. Under all the tested conditions, Δf never exceeds 1%. Clearly, the higher the frequency, the lower the deviation, since the window processed by the algorithm contains more signal cycles.

In Fig. 10 the amplitude deviation is shown. The most noticeable effect is the apparent periodicity of the estimation deviation with respect to the set frequency. This is due to the frequency response of the filter which exhibits the typical Gibbs effect oscillations. They are due to the tradeoff made in the filter design between the filter length and its performance. The filter effects have been partially compensated, but they persist in the final results. The deviation values are, however, within accepted limits for monitoring applications. It is noted that the estimation error is proportional to the absolute

TABLE I

ESTIMATES DEVIATION OBSERVED WITH CLASSICAL DMD AND DYNAMIC-ORDER DMD

Nominal values			Dynamic order (thr=0.97)			Dynamic order (thr=0.95)			Static order		
f [Hz]	A [Hz]	s[s-1]	Δf [%]	ΔA [%]	$\Delta\sigma$[%]	Δf [%]	ΔA [%]	$\Delta\sigma$[%]	Δf [%]	ΔA [%]	$\Delta\sigma$[%]
0.15	0.01	-0.01	0.62	2.40	12.84	0.73	8.21	21.46	1.73	79.52	81.43
0.15	0.01	0.001	0.64	2.54	15.12	0.75	9.44	20.18	3.19	72.73	73.15
0.15	0.01	0.01	0.62	2.02	4.33	0.72	9.25	21.81	1.50	73.65	82.59
0.15	0.05	-0.01	0.61	2.43	13.21	0.76	5.38	18.43	0.88	15.34	22.51
0.15	0.05	0.001	0.63	2.51	14.32	0.73	5.61	19.21	1.01	16.72	24.25
0.15	0.05	0.01	0.59	2.48	4.64	0.78	5.79	18.07	0.72	15.90	24.74
0.15	0.1	-0.01	0.62	2.39	12.54	0.71	6.15	19.02	0.81	17.23	24.52
0.15	0.1	0.001	0.63	2.21	14.67	0.74	5.93	18.76	1.04	16.68	23.41
0.15	0.1	0.01	0.60	2.42	4.23	0.78	6.06	19.43	0.95	16.13	22.67
0.25	0.01	-0.01	-0.72	7.26	-10.32	-0.91	13.65	-20.12	1.13	14.34	20.58
0.25	0.01	0.001	-0.71	6.81	-11.28	-0.88	13.93	-18.58	0.91	16.02	22.16
0.25	0.01	0.01	-0.72	7.02	-13.11	-0.84	15.77	-20.69	0.87	15.41	20.34
0.25	0.05	-0.01	-0.69	6.75	-11.16	-0.87	9.32	-17.32	0.78	10.11	-17.44
0.25	0.05	0.001	-0.71	6.71	-12.31	-0.93	10.21	-16.41	0.71	11.36	-16.92
0.25	0.05	0.01	-0.73	6.82	-13.48	-0.88	9.85	-17.07	0.83	10.52	-17.19
0.25	0.1	-0.01	-0.65	6.23	-10.44	-0.83	9.37	-17.42	0.64	6.42	-12.65
0.25	0.1	0.001	-0.66	6.55	-10.73	-0.84	9.64	-16.92	0.78	7.16	-15.74
0.25	0.1	0.01	-0.65	6.35	-11.85	-0.89	10.03	-16.75	0.77	6.94	-14.39
0.35	0.01	-0.01	-0.43	2.55	-2.12	-0.61	8.95	-10.43	0.76	18.42	-20.15
0.35	0.01	0.001	-0.41	2.46	-4.68	-0.64	9.67	-11.05	0.68	17.79	-21.87
0.35	0.01	0.01	-0.40	2.51	-5.47	-0.68	9.32	-10.97	0.71	17.34	-20.41
0.35	0.05	-0.01	-0.40	2.59	-1.89	-0.62	6.39	-6.12	0.63	15.48	-21.96
0.35	0.05	0.001	-0.41	2.55	-4.32	-0.63	6.88	-7.05	0.58	14.17	-21.51
0.35	0.05	0.01	-0.41	2.34	-5.16	-0.69	6.14	-6.11	0.59	15.63	-20.12
0.35	0.1	-0.01	-0.38	2.41	-1.05	-0.67	5.31	-5.96	0.61	5.23	-7.16
0.35	0.1	0.001	-0.39	2.39	-4.01	-0.65	6.03	-6.08	0.57	6.02	-8.13
0.35	0.1	0.01	-0.38	2.47	-4.86	-0.68	5.72	-6.41	0.59	5.11	-7.59

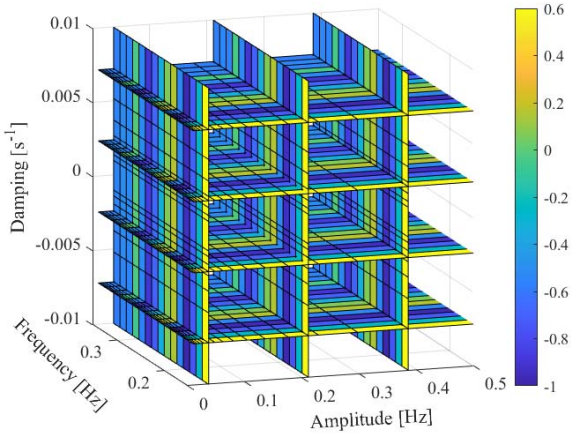

Fig. 9. Deviation of frequency estimates with single-oscillation signals.

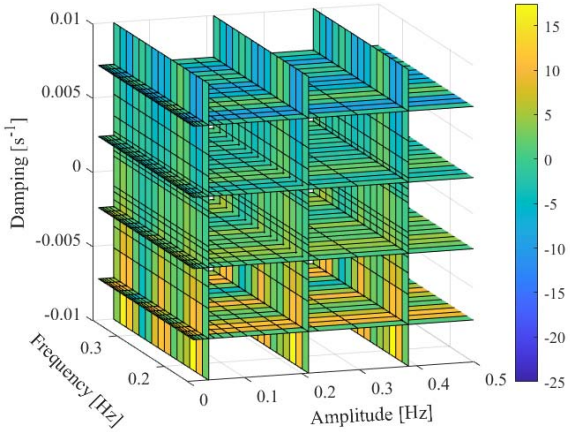

Fig. 10. Deviation of amplitude estimates with single-oscillation signals.

value of the damping; for strongly damped oscillations, the amplitude value is underestimated, while it is overestimated in the case of divergent oscillations. In the typical range of damping between -0.005 and 0.005, ΔA remains within 5%. Finally, the higher deviations (near to 25%) are observed when the amplitude value of the synthesized oscillation is lower than 0.02 Hz. For greater amplitudes, ΔA is within the range from -15% to 15%.

The deviation of the damping estimate is shown in Fig. 11. Again, a periodicity with the frequency of the oscillation can be seen, again due to the filter response. On the other hand, the damping estimate and amplitude are intimately related to each other. No significant effects related to the amplitude and damping of the input signal are observed. In each experiment, however, the $\Delta\sigma$ is less than 25%, i.e., absolute values less than 0.0025 s^{-1}.

To verify the performance guaranteed by the dynamic-order algorithm, the same tests were repeated with the classical DMD. Moreover, to show the different performance observed if the energy threshold value changes, the tests were repeated with the dynamic-order DMD, but with a threshold value equal to 95%. In Table I only some of the observed results are reported, for the sake of brevity. The shown values are the estimate deviations, as defined in (20). It can be noticed that the deviations of frequency estimates provided by the classical DMD are close to those granted by the dynamic-order algorithm. As regards the amplitude and damping estimates, the deviations observed for the classical algorithm exhibit values much higher than those provided by the dynamic-order DMD. This difference is mainly due to the mode mixing problem, which occurs especially when the signal amplitude is low. As regards the results observed with the threshold set to 0.95, higher estimates deviation is observed. In fact, according to the 0.97 threshold, four modes are always detected. With the 0.95 threshold, the number of detected modes varies from two to four; when the number of modes is less than four,

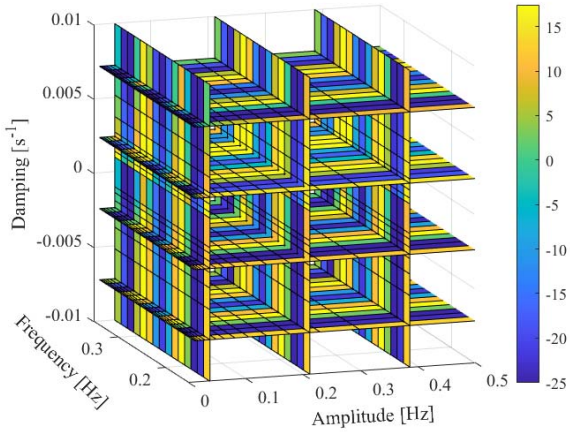

Fig. 11. Deviation of damping estimates with single-oscillation signals.

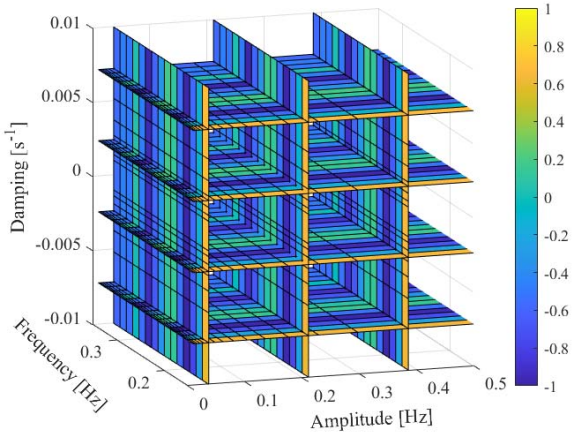

Fig. 12. Deviation of frequency estimates with two-oscillation signals.

an increase in the estimates deviation (especially as regards amplitude and damping) is observed.

A global assessment of performance has been also performed with two-oscillation signals. In particular, a signal was synthesized in which the first oscillation is characterized by fixed parameters (amplitude equal to 0.02 Hz, frequency equal to 0.1 Hz, and damping equal to 0.005 Hz), the second oscillation is characterized by parameters ranging in the same intervals used for the characterization with single-oscillation signals. The results obtained for Δf, ΔA, and $\Delta \sigma$ are shown, respectively, in Figs. 12–14.

It can be observed that the estimate deviations exhibit the same behavior than that appreciated with a single-oscillation signal. The deviations assume a slightly higher value, probably due to the interference related to the second component. In any case, even in the presence of two oscillations, the deviations of the estimates assume satisfactory values, especially with regard to the frequency and amplitude estimates.

VI. Assessment on Real WAMS Signals

The proposed method has been tested also with real signals, obtained from the WAMS of the Italian transmission network. For confidentiality issues, the names of the PMUs are not shown and the time labels have been changed with respect to the real transmitted timestamps.

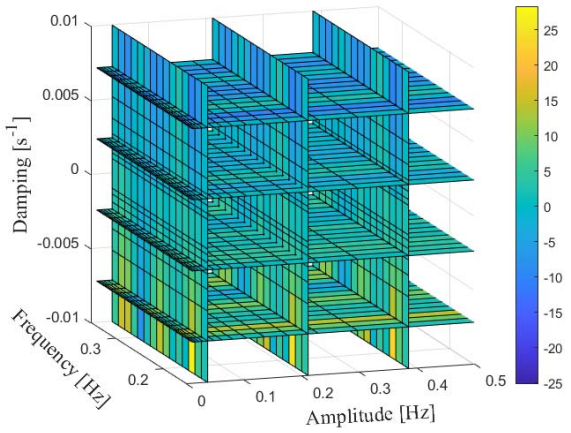

Fig. 13. Deviation of amplitude estimates with two-oscillation signals.

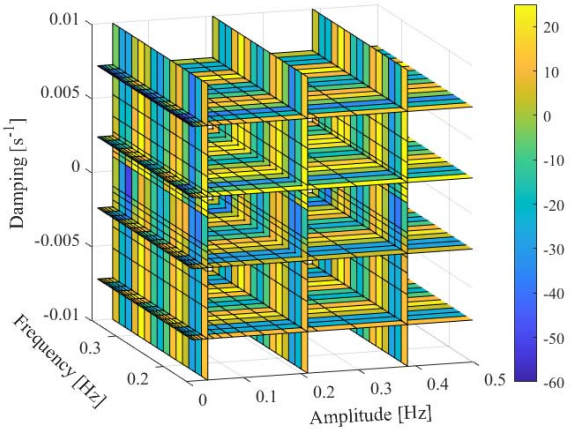

Fig. 14. Deviation of damping estimates with two-oscillation signals.

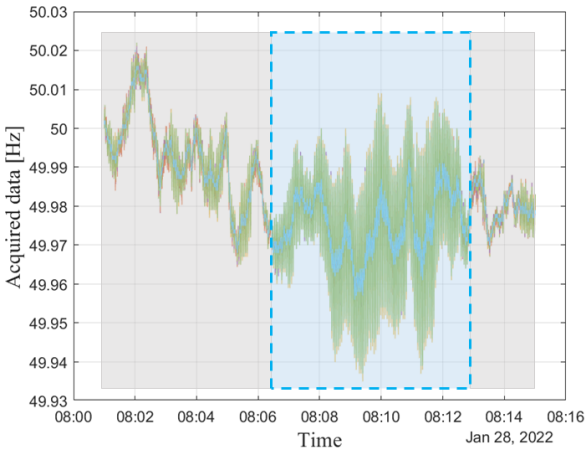

Fig. 15. Frequency measurement provided by WAMS: example 1.

An example of an event captured by the WAMS measurement systems is shown in Fig. 15. Compared to the synthesized signal, it has to be considered that the actual signal in most of the observation time does not exhibit significant oscillations. Therefore, the signal presents some zones, referred to as ambient data, in which there is only noise. The areas called transient data, instead, are the intervals in which oscillatory phenomena are present. In Fig. 15, the ambient data have been highlighted with gray rectangles and the transient data have been highlighted with a blue rectangle. In Fig. 16(a) and (b), the estimates of frequency and damping obtained by the

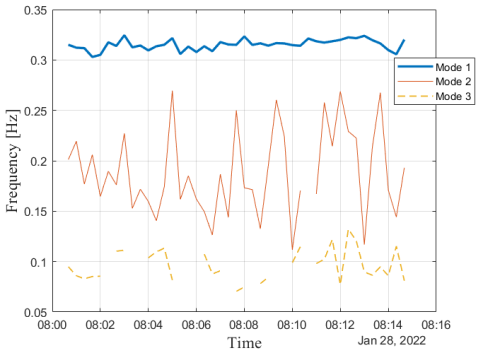

(a)

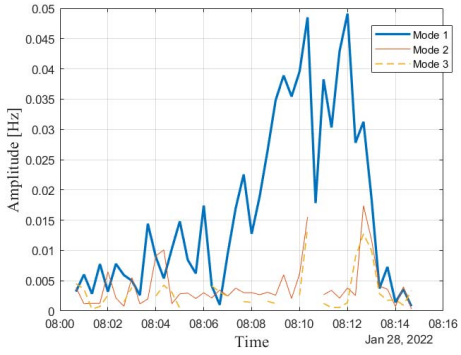

(b)

Fig. 16. Estimated parameters for the WAMS signal in Fig. 15 with classical DMD. (a) Estimated frequency. (b) Estimated amplitude.

classical algorithm with static order are shown, respectively. Even on the real data, the phenomenon of mode mixing is observed, so that, in some windows, the amplitude of mode 1 is attributed to mode 2. The classical DMD does not make a difference between ambient data and transient data, since it tries to reconstruct always the same number of modes. The damping has not been reported, because when the mode mixing occurs, damping estimates are not significant.

The frequency, amplitude, and damping estimates obtained by the proposed method are shown in Fig. 17. Here it can be observed that the measurement algorithm behaves differently depending on whether it processes ambient data or transient data.

In ambient data, since there are no predominant modes, the order at which the CSSV exceeds 97% of the total amplitude of the singular values can also be very high (between 15 and 18); in fact, the contribution of each singular value to the information content of the signal is negligible. To avoid the representation of such a high number of modes, that are also non-significant, the maximum value of the order was forced to 8, so that the algorithm returns the same output of the DMD with static order.

Another issue concerns the damping estimates on the ambient data. Clearly, these estimates are non-significant; so, to avoid getting wrong information from the damping observation, the damping estimates are not plotted if the corresponding mode amplitude is less than 0.01 Hz. Clearly, this solution cannot also be used for classical DMD because, due to mode mixing, amplitude estimates are not always reliable.

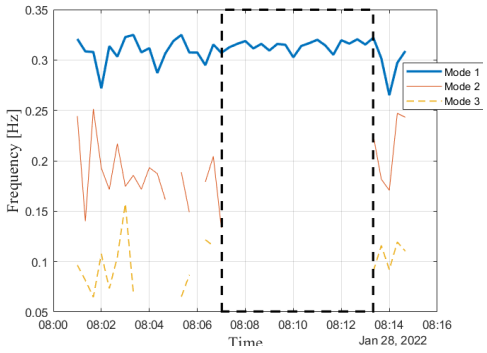

(a)

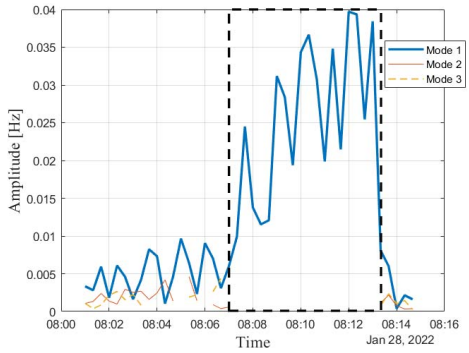

(b)

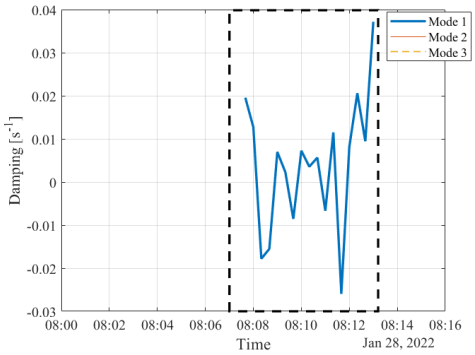

(c)

Fig. 17. Estimated parameters for the WAMS signal in Fig. 15 with the proposed method. (a) Estimated frequency. (b) Estimated amplitude. (c) Estimated damping.

The notable difference between the proposed method and classical DMD can be appreciated on the transient data. Dynamic-order DMD effectively focuses on the dominant mode which, this time, represents most of the information content of the signal; the oscillatory mode is correctly recognized and a single estimate of amplitude, frequency, and damping associated with the only recognized mode is obtained.

It can be seen from the figures that the amplitude estimate reproduces quite faithfully the envelope of the acquired signal. Also the values of the estimates are consistent with the peak-to-peak amplitude of the oscillations observed in Fig. 15. Also the damping estimates are consistent with the raw data, since negative values are observed in correspondence of the time windows in which the amplitude of the oscillations increases.

Another example of the method reliability is given on the signal shown in Fig. 18.

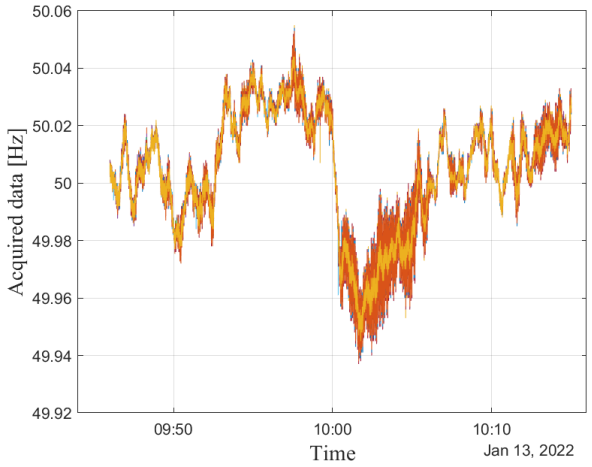

Fig. 18. Acquired frequency measures.

The corresponding estimated parameters are shown in Fig. 19. Again, the zone where a transient is occurring is immediately identified, as the algorithm determines only one dominant mode, of frequency equal to 0.28 Hz. The amplitude estimate effectively follows the peak-to-peak amplitude of the acquired signal, and the damping estimate highlights the time windows in which the oscillation is diverging with good reliability.

It is worth pointing out that this analysis is off-line, so it is not subject to time-criticality issues; the authors, then, were able to compare the obtained frequency estimates with the output provided by algorithms typically adopted for frequency trajectory estimation, such as short time Fourier transform (STFT) and WT. A relevant agreement of the values has been appreciated.

VII. Conclusion

In this article, a new method for the analysis of inter-area oscillations on transmission networks is proposed. The method exploits the modal analysis performed by the DMD algorithm. However, traditional DMD has a limitation related to the selection of the order to which the matrix of the singular value should be reduced. The proposed algorithm overcomes this limitation, as it automatically identifies the optimal order, on the basis of the energy content of the input signal.

The proposed method has been characterized through several tests, with both synthesized signals and signals actually acquired by WAMS. The former was performed in MATLAB environment, synthesizing signals consisting of one or two oscillations and varying the amplitude, frequency, and damping parameters. In all tests, there was a significant improvement in performance compared to the classic DMD algorithm, which, in the presence of noise, suffers from the problem of mode mixing and makes the estimates of amplitude unreliable.

Simulated tests have shown that the proposed algorithm has excellent accuracy in frequency estimation; the deviation between estimated and nominal value, in all tests, is never greater than 1%.

The amplitude estimation also presents satisfactory accuracy. If the synthesized oscillation is not too attenuated

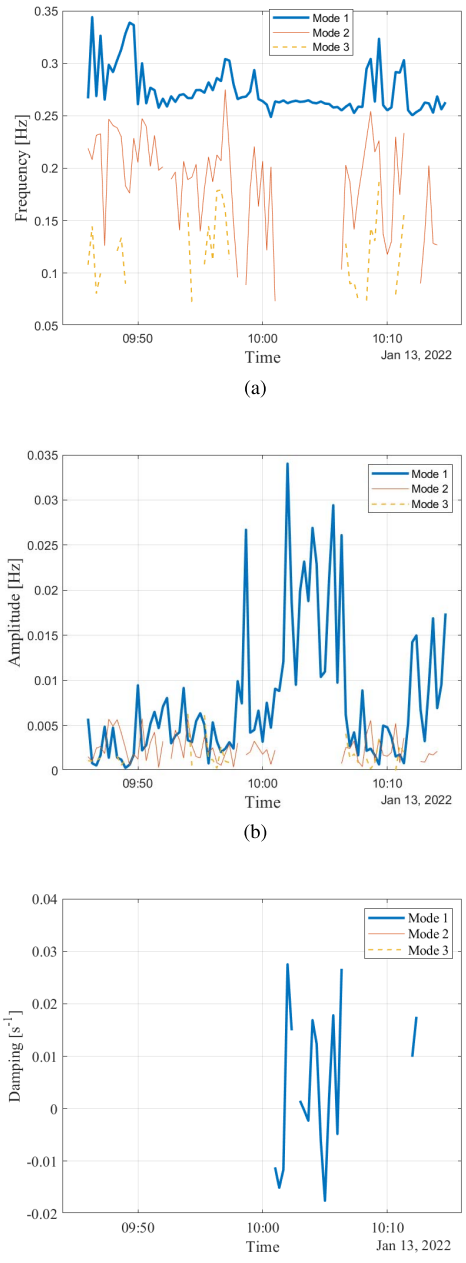

Fig. 19. Estimated parameters for WAMS signal in Fig. 18 with the proposed method. (a) Estimated frequency. (b) Estimated amplitude. (c) Estimated damping.

(amplitude greater than 0.02), the deviation of the amplitude estimate remains within the range of 15%.

Damping is the parameter with the highest deviations, although they are still lower than 30% if the amplitude of the synthesized signal is not too low.

Tests conducted on real frequency measurements from the WAMS confirmed the reliability observed in the simulated tests.

The obtained results suggest that the proposed method exhibits excellent performance in the real-time analysis of the oscillatory transient. By means of a trigger on the amplitude estimation, it is possible to early detect dangerous oscillations and take the proper countermeasures. On the other hand,

a good damping estimation allows to recognize in advance the behavior of the oscillation, so it would be advisable to improve the accuracy guaranteed by the proposed method. To this end, the authors are going to evaluate the possibility of combining dynamic-order DMD with other approaches more specialized to damping estimation. Dynamic-order DMD would be used to estimate frequency and amplitude; the estimates could be the input for a successive algorithm that only needs to estimate damping and refine the amplitude estimate accordingly.

REFERENCES

[1] P. Kundur *et al.*, "Definition and classification of power system stability IEEE/CIGRE joint task force on stability terms and definitions," *IEEE Trans. Power Syst.*, vol. 19, no. 3, pp. 1387–1401, May 2004.

[2] P. S. Kundur, "Power system stability," in *Power System Stability and Control*. Boca Raton, FL, USA: CRC Press, 2017, pp. 1–8.

[3] M. Mansouri, M. Mojiri, M. A. Ghadiri-Modarres, and M. Karimi-Ghartemani, "Estimation of electromechanical oscillations from phasor measurements using second-order generalized integrator," *IEEE Trans. Instrum. Meas.*, vol. 64, no. 4, pp. 943–950, Apr. 2015.

[4] G. Rogers, *Power System Oscillations*. Berlin, Germany: Springer, 2012.

[5] A. R. Messina, *Inter-Area Oscillations in Power Systems: A Nonlinear and Nonstationary Perspective*. Berlin, Germany: Springer, 2009.

[6] G. Giannuzzi, D. Lauria, C. Pisani, and D. Villacci, "Real-time tracking of electromechanical oscillations in ENTSO-e continental European synchronous area," *Int. J. Electr. Power Energy Syst.*, vol. 64, pp. 1147–1158, Jan. 2015.

[7] D. Cirio, D. Lucarella, G. Giannuzzi, and F. Tuosto, "Wide area monitoring in the Italian power system: Architecture, functions and experiences," *Eur. Trans. Electr. Power*, vol. 21, no. 4, pp. 1541–1556, May 2011.

[8] L. Michi, G. Giannuzzi, C. Pisani, E. M. Carlini, and R. Zaottini, "Improving dynamic stability in presence of static generation: Issues and potential countermeasures," in *Proc. AEIT Int. Annu. Conf. (AEIT)*, Sep. 2019, pp. 1–6.

[9] C. Muscas *et al.*, "Characterization of a PMU-based method for transmission line parameters estimation with systematic measurement error modeling," in *Proc. AEIT Int. Annu. Conf. (AEIT)*, Oct. 2021, pp. 1–6.

[10] P. Tosato, D. Macii, M. Luiso, D. Brunelli, D. Gallo, and C. Landi, "A tuned lightweight estimation algorithm for low-cost phasor measurement units," *IEEE Trans. Instrum. Meas.*, vol. 67, no. 5, pp. 1047–1057, May 2018.

[11] A. Berizzi *et al.*, "Real-time identification of electromechanical oscillations through dynamic mode decomposition," *IET Gener., Transmiss. Distrib.*, vol. 14, no. 19, pp. 3992–3999, Oct. 2020.

[12] "Analysis of CE inter-area oscillations of 19th and 24th febbraio 2011," Eur. Netw. Transmiss. Syst. Oper. Electr., Brussel, Belgium, Tech. Rep., 2011. [Online]. Available: https://eepublicdownloads.entsoe.eu/clean-documents/pre2015/publications/entsoe/RG_SOC_CE/Top7_110913_CE_inter-area-oscil_feb_19th_24th_final.pdf

[13] "Analysis of CE inter-area oscillations of 1st December 2016," Eur. Netw. Transmiss. Syst. Oper. Electr. (ENTSO-E), Brussel, Belgium, Tech. Rep., 2017. [Online]. Available: https://eepublicdownloads.entsoe.eu/clean-documents/SOCdocuments/Regional Groups Continental Europe/2017/CEinter-area oscillations Dec 1st 2016 PUBLIC V7.pdf

[14] H. Zamani, M. Karimi-Ghartemani, and M. Mojiri, "Analysis of power system oscillations from PMU data using an EPLL-based approach," *IEEE Trans. Instrum. Meas.*, vol. 67, no. 2, pp. 307–316, Feb. 2018.

[15] M. I. Hossain, M. Shafiullah, M. Abido, and M. Al Emran, "Online monitoring of inter-area oscillations and damping of power systems employing Prony analysis," in *Proc. 10th Int. Conf. Electr. Comput. Eng. (ICECE)*, Dec. 2018, pp. 269–272.

[16] P. Ray, "Power system low frequency oscillation mode estimation using wide area measurement systems," *Eng. Sci. Technol., Int. J.*, vol. 20, no. 2, pp. 598–615, Apr. 2017.

[17] X. Xia, C. Li, and W. Ni, "Dominant low-frequency oscillation modes tracking and parameter optimisation of electrical power system using modified Prony method," *IET Gener., Transmiss. Distrib.*, vol. 11, no. 17, pp. 4358–4364, Nov. 2017.

[18] R. Kumaresan and D. Tufts, "Estimating the parameters of exponentially damped sinusoids and pole-zero modeling in noise," *IEEE Trans. Acoust., Speech, Signal Process.*, vol. ASSP-30, no. 6, pp. 833–840, Dec. 1982.

[19] M. E. Magana and A. Kandukuri, "Non-data-aided parametric- and nonparametric-based carrier frequency estimators for burst GMSK communication systems," *IEEE Trans. Instrum. Meas.*, vol. 59, no. 7, pp. 1783–1792, Jul. 2010.

[20] M. Barbosh, P. Singh, and A. Sadhu, "Empirical mode decomposition and its variants: A review with applications in structural health monitoring," *Smart Mater. Struct.*, vol. 29, no. 9, Sep. 2020, Art. no. 093001.

[21] F. Bonavolontà, L. P. Di Noia, D. Lauria, A. Liccardo, and S. Tessitore, "An optimized HT-based method for the analysis of inter-area oscillations on electrical systems," *Energies*, vol. 12, no. 15, p. 2935, Jul. 2019.

[22] D. Lauria and C. Pisani, "On Hilbert transform methods for low frequency oscillations detection," *IET Gener., Transmiss. Distrib.*, vol. 8, no. 6, pp. 1061–1074, Jun. 2014.

[23] F. Bonavolontà, L. P. D. Noia, A. Liccardo, S. Tessitore, and D. Lauria, "A PSO-MMA method for the parameters estimation of interarea oscillations in electrical grids," *IEEE Trans. Instrum. Meas.*, vol. 69, no. 11, pp. 8853–8865, Nov. 2020.

[24] Y. Sun, Y. Wang, L. Bai, Y. Hu, D. Sidorov, and D. Panasetsky, "Parameter estimation of electromechanical oscillation based on a constrained EKF with CI-PSO," *Energies*, vol. 11, no. 8, p. 2059, Aug. 2018.

[25] Y. Wang, Y. Sun, Z. Wei, and G. Sun, "Parameters estimation of electromechanical oscillation with incomplete measurement information," *IEEE Trans. Power Syst.*, vol. 33, no. 5, pp. 5016–5028, Sep. 2018.

[26] J. C.-H. Peng and N.-K. C. Nair, "Enhancing Kalman filter for tracking ringdown electromechanical oscillations," *IEEE Trans. Power Syst.*, vol. 27, no. 2, pp. 1042–1050, May 2012.

[27] J. L. Rueda, C. A. Juárez, and I. Erlich, "Wavelet-based analysis of power system low-frequency electromechanical oscillations," *IEEE Trans. Power Syst.*, vol. 26, no. 3, pp. 1733–1743, Aug. 2011.

[28] F. Shiri and B. Mohammadi-Ivatloo, "Identification of inter-area oscillations using wavelet transform and phasor measurement unit data," *Int. Trans. Electr. Energy Syst.*, vol. 25, no. 11, pp. 2831–2846, Nov. 2015.

[29] T. Jiang, L. Bai, G. Li, H. Jia, Q. Hu, and H. Yuan, "Estimating inter-area dominant oscillation mode in bulk power grid using multi-channel continuous wavelet transform," *J. Mod. Power Syst. Clean Energy*, vol. 4, no. 3, pp. 394–405, Jul. 2016.

[30] P. Zhang, Y. Teng, X. Wang, and X. Wang, "Estimation of interarea electromechanical modes during ambient operation of the power systems using the RDT–ITD method," *Int. J. Electr. Power Energy Syst.*, vol. 71, pp. 285–296, Oct. 2015.

[31] D. Cai, P. Regulski, M. Osborne, and V. Terzija, "Wide area inter-area oscillation monitoring using fast nonlinear estimation algorithm," *IEEE Trans. Smart Grid*, vol. 4, no. 3, pp. 1721–1731, Sep. 2013.

[32] S. A. N. Sarmadi and V. Venkatasubramanian, "Inter-area resonance in power systems from forced oscillations," *IEEE Trans. Power Syst.*, vol. 31, no. 1, pp. 378–386, Jan. 2016.

[33] J. N. Kutz, S. L. Brunton, B. W. Brunton, and J. L. Proctor, *Dynamic Mode Decomposition: Data-Driven Modeling of Complex Systems*. Philadelphia, PA, USA: SIAM, 2016.

[34] P. J. Schmid and J. Sesterhenn, "Dynamic mode decomposition of experimental data," in *Proc. 8th Int. Symp. Part. Image Velocimetry*, Melbourne, VIC, Australia, 2009, pp. 1–4.

[35] P. J. Schmid, "Dynamic mode decomposition of numerical and experimental data," *J. Fluid Mech.*, vol. 656, pp. 5–28, Jan. 2010.

[36] "Image processing toolbox user's guide," MathWorks, Natick, MA, USA, Tech. Rep., 2021. [Online]. Available: https://it.mathworks.com/help/pdf_doc/images/images_ug.pdf

[37] J. N. Kutz, X. Fu, and S. L. Brunton, "Multiresolution dynamic mode decomposition," *SIAM J. Appl. Dyn. Syst.*, vol. 15, no. 2, pp. 713–735, 2016.

Annalisa Liccardo received the M.S. *(cum laude)* and Ph.D. degrees in electrical engineering from the University of Naples Federico II, Naples, Italy, in 2003 and 2006, respectively.

She was a Tenure Track Researcher with the Department of Electrical Engineering and Information Technology, University of Naples Federico II, from 2013 to 2016, where she has been an Associate Professor since 2016. She has founded the Spin off ARCADIA, Naples, Italy, for the realization of AR environments for remote control of measurement instruments. Her main current research interests involve advanced measurements for monitoring and protection of electrical power systems, the IoT sensors for electrical measurements, distributed measurement systems, and AR-based remote laboratory.

Salvatore Tessitore received the B.Sc. and M.Sc. degrees in electrical engineering from the University of Naples Federico II, Naples, Italy, in 2016 and 2019, respectively, where he is currently pursuing the Ph.D. degree with the School of Information Technology and Electrical Engineering.

He is currently with Terna Rete Italia spa, Rome, Italy. His research activity concerns measurements and signal processing for electrical transmission networks.

Francesco Bonavolontà received the master's and the Ph.D. degrees in electrical engineering from the University of Naples Federico II, Naples, Italy, in 2011 and 2015, respectively.

He is currently a Research Fellow with the Department of Electrical and Information Technologies, University of Naples Federico II. He has founded the Spin off ARCADIA, for the realization of AR environments for remote control of measurement instruments. He has received the National License as an Associate Professor of the scientific area 09/E4 measurements. His research activity is centered in the area of instrumentation and measurement and can be divided into three main areas: remote control of measurement instruments, measurement methods based on compressive sampling, and distributed measurement systems for monitoring and protecting electrical networks. More recently its research activities are focusing on the development of innovative measurement sensors based on artificial intelligence algorithms.

Dr. Bonavolontà is a member of the Technical Commitee TC-37-Measurements and Networking of IEEE.

Sara Cristiano received the M.S. degree in electrical engineering from the University of Naples Federico II, Naples, Italy, in 2021.

She joined two Erasmus programs at the University of Applied Sciences–Fachhochschule Südwestfalen of Soest (NRW), Soest, Germany, and the Technical University of Munich (TUM), Munich, Germany. She received the research grant from the University of Naples Federico II concerning the IoT-based measurement system for the infrastructure monitoring. Since June, she has been with the Stability and Network Logics Team, Dispatching and Switching Department, TERNA, Rome, Italy.

Luigi Pio Di Noia (Senior Member, IEEE) received the M.S. and Ph.D. degrees in electrical engineering from the University of Naples Federico II, Naples, Italy, in 2011 and 2015, respectively.

Since 2018, he has been a Research Fellow of electrical machines, power electronics and electric drives with the University of Naples Federico II. His research interests include the design and control of electrical machines and drives for aerospace and traction, the development of fault diagnosis, and prognostic algorithms for electrical drives.

Giorgio Maria Giannuzzi received the master's degree in electrical engineering from the University of Rome, Rome, Italy, in 1996.

Until December 2000, he has worked with ABB, Zürich, Switzerland, where he was in charge of network studies, protection and control applications, with special reference to RTU apparatus and data engineering issues. Since 2001, he has been working with TERNA, Rome, as an Expert in defense plans/systems, dynamic studies, protection, telecontrol and substation automation. From 2004 to 2011, he coordinated the study, design and activation of wide area defense system (including interruptible customers system) and wide area monitoring system. In addition, under his guidance, the main security energy management systems were designed and coded: they are actually in use at the National Control Centre (optimal power flow security and market constrained, optimal reactive power flow, dynamic security assessment tool, dynamic and static security verification software, operator training simulator). He has supervised the revision of main Italian grid code technical enclosures (primary and secondary frequency regulation, load shedding, protection and automation, and defense plans). Until 2009, he was a member of a UCTE Expert Group on Power System Stability. In 2010, he joined ENTSO-E, Bruxells, Belgium, System Protection and Dynamics Group, where he is the Convenor, starting from 2014, coordinating the European evaluation over dispersed generation impact on system security and load shedding guidelines. He is currently responsible of the Engineering Department, National Dispatching Centre.

Cosimo Pisani received the Ph.D. degree in electrical engineering from the University of Naples Federico II, Naples, Italy, in 2014.

During his Ph.D. degree in collaboration with TERNA, Rome, Italy, he investigated some dynamic stability issues of large interconnected power system, such as the European one. He is currently the Head of Stability and Network Logics at the Dispatching and Switching Department. He is the author or a coauthor of more than 80 scientific articles in IEEE e CIGRE community. His research interests include applications of dynamic stability of power systems, wide area monitoring and protection systems, high-voltage direct current systems, and power system restoration. He is the Leader of wide area monitoring system (WAMS) task force within ENTSO-E System Protection and Dynamic and Italian representative of CIGRE Study Committee C4 System Technical Performance.